CEBAF PR-93-011
June 1993

Automated Measurement of Cavity Frequency and Cavity Tuning at CEBAF

R. Li, S. Simrock, B. Yunn
Continuous Electron Beam Accelerator Facility
12000 Jefferson Avenue
Newport News, VA 23606

CONTINUOUS
ELECTRON
BEAM
ACCELERATOR
FACILITY

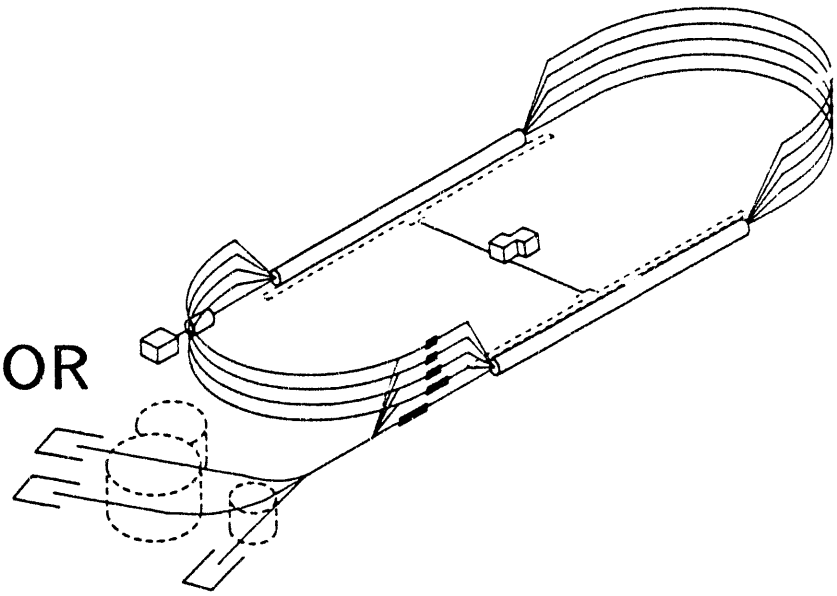

SURA SOUTHEASTERN UNIVERSITIES RESEARCH ASSOCIATION

CEBAF

Newport News, Virginia

Copies available from:

Library
CEBAF
12000 Jefferson Avenue
Newport News
Virginia 23606

The Southeastern Universities Research Association (SURA) operates the Continuous Electron Beam Accelerator Facility for the United States Department of Energy under contract DE-AC05-84ER40150.

Automated Measurement of Cavity Frequency and Cavity Tuning at CEBAF*

Rui Li, Stefan N. Simrock and Byung C. Yunn
CEBAF, 12000 Jefferson Ave., Newport News, VA 23606

Abstract

We propose a method here which allows the measurement of the cavity resonance frequency in a frequency range up to ±5 kHz from the operating frequency. This is achieved by phase modulation of the incident signal with noise to drive the cavity with a broad band spectrum. The cavity resonance frequency can then be determined from the response signal of the field probe, which has a narrow frequency spectrum due to the high loaded Q of the cavity of 6.6×10^6, corresponding to a cavity bandwidth of 125 Hz.

Introduction

The cavity tuning algorithms as presently implemented in the CEBAF RF control system rely on the accuracy of the detuning angle measurements. It is measured as the phase difference between the incident and transmitted RF power and due to hardware limitations not accurate at low-power levels, i.e., if the cavity is detuned by several bandwidths or at very low gradients. Phase offsets are changing as functions of temperature and power level or replacement of control modules. In many instances cavities need to be tuned manually after accelerator shutdown. In this study, we propose a method to measure the cavity resonance freqency by driving the cavity with a noise spectrum. This is achieved by modulating the phase of the incident signal with a band-limited pseudo-random signal. The cavity resonance frequency can then be determined from the response signal of the field probe, which has a narrow frequency spectrum due to the high loaded Q of the cavity of 6.6×10^6, corresponding to a cavity bandwidth of 125 Hz. The presently used hardware allows the measurement of the cavity frequency in a range up to ±5 kHz from the operating frequency.

Layout of the Scheme

The principle of the scheme is shown in Fig. 1. A signal $V_1(t) = |V_1|e^{-i\omega_0 t}$ from the master oscillator (A) is sent to a vector modulator (B), where $V_1(t)$ is modulated by a pseudo random signal $x(t) = e^{i\phi(t)}$. The power spectrum of $x(t)$ is required to be a positive constant for $|f| < 5$ kHz and to be zero outside this frequency region. The output signal from (B) $V_{\rm in}(t) = V_1(t)x(t)$ is then sent to the cavity (C), which excites the cavity at its resonance frequency f_c (assuming $|f_c - f_0| < 5$ kHz with $f_0 = \omega_0/2\pi$). A sample of the accelerating field $V_c(t)$, as the response to the incident signal $V_{\rm in}(t)$, is detected by the probe coupler. Then at the vector demodulator (D) the signal $V_c(t)$ is multiplied by a reference signal $V_2(t) = |V_2|e^{i\omega_0 t}$ from the master oscillator to generate a baseband signal $y(t) = V_2(t)V_c(t)$. Our task is to generate a bandwidth-limited signal $x(t)$ at the vector modulator (B), and then set a scheme to detect the cavity resonance frequency f_c from the signal $y(t)$ ouput from the vector demodulator (D).

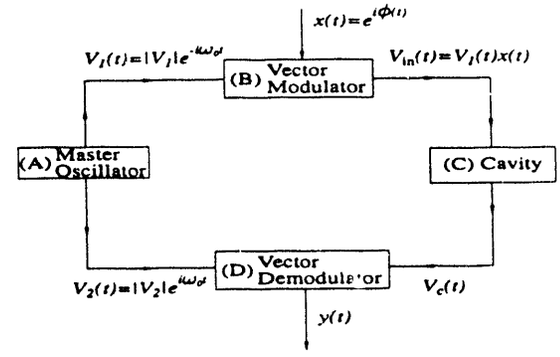

Figure 1: Layout of the cavity resonance frequency measurement scheme.

Generation of a Bandwidth-Limited Random Signal

First, a real ideal bandwidth-limited signal $u(t)$ for $0 < t < T$, whose power spectrum $S_{uu}(\omega)$ satisfies

$$S_{uu}(\omega) = \begin{cases} S_0 & |\omega| < \omega_b \\ 0 & |\omega| > \omega_b \end{cases}, \qquad (1)$$

is generated using the sampling theorem [1]:

$$u(t) = \sum_{n=-N_1}^{N_2} u(nT_b) \frac{\sin \omega_b(t - nT_b)}{\omega_b(t - nT_b)} \qquad (0 < t < T) \qquad (2)$$

with $T_b = 2\pi/\omega_b$. Here $u_n = u(nT_b)$ are uniformly distributed in the range $(-1, 1)$, and n runs from $-N_1$ to N_2, with $(T_1, T_2) = (-N_1 T_b, N_2 T_b)$ fully covering the time range $t = (0, T)$.

Let u and v be both ideal bandwidth-limited real pseudo-random processes independently generated using Eq. (2), and define a complex signal $w(t)$

$$w(t) = u(t) + iv(t). \qquad (3)$$

It can be shown that $w(t)$ is an ideal bandwidth-limited signal. We can write $w(t)$ in terms of the amplitude and the phase

$$w(t) = |w(t)|e^{i\phi(t)}. \qquad (4)$$

*Supported by D.O.E. contract #DE-AC05-84ER40150

Numerically it turns out that the signal formed from the phase variation of $w(t)$ only, namely,

$$x(t) = e^{i\phi(t)} = w(t)/|w(t)| \tag{5}$$

is also a good approximation of a bandwidth-limited signal. This is shown in Fig. 2.

Response Signal from the Cavity

The analysis for the output signal $y(t)$ of the overall system is given in this section.

The pseudo random signal $x(t)$ is multiplied by the signal $V_1(t)$ from the master oscillator at the vector modulator (B), producing an incident signal $V_{\rm in}(t)$ to the cavity,

$$V_{\rm in}(t) = V_1(t)x(t). \tag{6}$$

The cavity (C) acts like a forced oscillator with characteristic resonance angular frequency ω_c and damping constant α. For an input signal $V_{\rm in}(t)$, the cavity probe will detect a gradient $V_c(t)$ which satisfies

$$\ddot{V}_c + 2\alpha\dot{V}_c + \omega_c^2 V_c = \lambda V_{\rm in}(t) \tag{7}$$

with λ containing the proper units. Assuming $V_c(0) = \dot{V}_c(0) = 0$ and applying Laplace transform to Eq. (7), we get

$$\begin{aligned} V_c(t) &= \frac{\lambda}{\omega_c'}\int_0^t e^{-\alpha(t-t')}\sin\omega_c'(t-t')\,V_{\rm in}(t')\,dt' \\ &\approx \frac{\lambda}{\omega_c}\int_0^t e^{-\alpha(t-t')}\sin\omega_c(t-t')\,V_{\rm in}(t')\,dt' \end{aligned} \tag{8}$$

with $\omega_c' = \sqrt{\omega_c^2 - \alpha^2}$. Here the relation $\alpha/\omega_c = 1/2Q_c \ll 1$ is used in Eq. (8) (Q_c is the effective quality value of the cavity). The response signal $V_c(t)$ from the cavity is then multiplied by $V_2(t)$ from the master oscillator at the vector demodulator (D), which gives

$$y_1 = V_2(t)V_c(t). \tag{9}$$

Combining Eqs. (6), (8) and (9), we get

$$y_1(t) = \frac{\lambda V_2(t)}{\omega_c}\int_0^t e^{-\alpha(t-t')}\sin\omega_c(t-t')V_1(t')x(t')\,dt'. \tag{10}$$

Together with $V_1(t) = |V_1|e^{-i\omega_0 t}$ and $V_2(t) = |V_2|e^{i\omega_0 t}$, one obtains

$$y_1(t) = a_1\int_0^t e^{-\alpha(t-t')}e^{i\omega_0(t-t')}\sin\omega_c(t-t')x(t')\,dt'. \tag{11}$$

Here $a_1 = \lambda|V_1V_2|/\omega_c$ is a constant. Denote $\tilde{\omega}_c$ as the cavity resonance frequency relative to ω_0, $\tilde{\omega}_c = \omega_c - \omega_0$, and assume the overall output signal $y(t)$ from the vector demodulator (D) extracts from $y_1(t)$ only the part containing the difference of the frequencies. It then yields

$$y(t) = a\int_0^t e^{-\alpha(t-t')}e^{-i\tilde{\omega}_c(t-t')}x(t')\,dt' \tag{12}$$

with constant $a = a_1/2i$. By taking the first derivative of $y(t)$ in Eq. (12) with respect to t, one can readily show that

$$\dot{y}(t) + (\alpha + i\tilde{\omega}_c)y(t) = a\,x(t). \tag{13}$$

Given ω_c, and thus knowing $\tilde{\omega}_c$, we can numerically integrate Eq. (13) to obtain $y(t)$ in terms of $x(t)$ as the simulation of the response signal of the whole system.

Let the Fourier transform of the processes $x(t)$ and $y(t)$ be $X(\omega)$ and $Y(\omega)$ respectively,

$$X(\omega) = \int_{-\infty}^{\infty} x(t)e^{-i\omega t}\,dt \text{ and } Y(\omega) = \int_{-\infty}^{\infty} y(t)e^{-i\omega t}\,dt. \tag{14}$$

From Eq. (13) one gets

$$Y(\omega) = \frac{aX(\omega)}{-i(\omega - \tilde{\omega}_c) + \alpha}. \tag{15}$$

The power spectra for the two processes are related by

$$S_{yy}(\omega) = \frac{|a|^2 S_{xx}(\omega)}{(\omega - \tilde{\omega}_c)^2 + \alpha^2}. \tag{16}$$

Power Spectrums

It shows below that an estimate of the cavity resonance frequency can be yielded from the proper averaging over the power spectrum of the output signal $y(t)$.

In real measurements, the signal lasts only for a finite time period. The Fourier transform of the process $y(t)$ for $0 < t < T$ is

$$Y(\omega) = \int_0^T y(t)e^{-i\omega t}. \tag{17}$$

It can be shown that

$$|Y(\omega)|^2 = \int_{-T}^{T} e^{-i\omega\tau}T(1 - \frac{|\tau|}{T})\langle R_{yy}(\tau)\rangle_T\,d\tau, \tag{18}$$

where $\langle R_{yy}(\tau)\rangle_T$ is the finite time correlation function

$$\langle R_{yy}(\tau)\rangle_T = \frac{1}{T-|\tau|}\cdot\begin{cases} \displaystyle\int_0^{T-|\tau|} y(t)y^*(t+|\tau|)\,dt & (\tau < 0) \\ \displaystyle\int_0^{T-\tau} y^*(t)y(t+\tau)\,dt & (\tau > 0). \end{cases} \tag{19}$$

Applying a convolution to the integral in Eq. (18), one has

$$|Y(\omega)|^2 \approx \frac{1}{2\pi}\int_{-\infty}^{\infty} T\left(\frac{\sin(\omega-\omega')T/2}{(\omega-\omega')T/2}\right)^2 S_{yy}(\omega')\,d\omega'. \tag{20}$$

Here it is assumed $\langle R_{yy}(\tau)\rangle_T \approx R_{yy}(\tau)$, and $S_{yy}(\omega)$ is the power spectrum

$$S_{yy}(\omega) = \int_{-\infty}^{\infty} R_{yy}(\tau)e^{-i\omega\tau}\,d\tau \tag{21}$$

with the correlation function $R_{yy}(\tau)$ obtained by averaging over infinite random ensembles

$$R_{yy}(\tau) = \langle R_{yy}(\tau)\rangle_{t\to\infty}. \tag{22}$$

The expression of $|Y(\omega)|^2$ in Eq. (20) corresponds to viewing the actual spectrum $S_{yy}(\omega)$ through a spectral window $W_T(\omega)$

$$W_T(\omega) = \frac{T}{2\pi}\left(\frac{\sin \omega T/2}{\omega T/2}\right)^2, \tag{23}$$

which provides a resolution of $\delta\omega = 2\pi/T$ [2]. Note $\lim_{T\to\infty} W_T(\omega) = \delta(\omega)$.

The above results can be further generalized to view $S_{yy}(\omega)$ at any resolution $\delta\omega > 2\pi/T$ by setting a cut-off to the correlation time range. Given T_M ($T_M < T$), the spectrum with resolution $\delta\omega = 2\pi/T_M$ is obtained by changing the integration range in Eq. (18) from $(-T, T)$ to $(-T_M, T_M)$,

$$\begin{aligned}\left[|Y(\omega)|^2\right]_{\delta\omega=2\pi/T_M} &= \int_{-T_M}^{T_M} e^{-i\omega\tau} T_M\left(1-\frac{|\tau|}{T_M}\right)\langle R_{yy}(\tau)\rangle_T \, d\tau \qquad (24)\\ &\approx \int_{-\infty}^{\infty} W_{T_M}(\omega-\omega') S_{yy}(\omega')\, d\omega'. \qquad (25)\end{aligned}$$

Combining Eq. (25) with Eq. (16), one gets

$$\left[|Y(\omega)|^2\right]_{\delta\omega=2\pi/T_M} \approx |a|^2 \int_{-\infty}^{\infty} \frac{W_{T_M}(\omega-\omega') S_{xx}(\omega')}{(\omega'-\tilde{\omega}_c)^2+\alpha^2}\, d\omega'. \tag{26}$$

Note $\left[|Y(\omega)|^2\right]_{\delta\omega=2\pi/T_M}$ samples $S_{xx}(\omega)$ at the frequency $\omega = \tilde{\omega}_c$ with width $\Delta\omega = \alpha$ and resolution $\delta\omega = 2\pi/T_M$.

When the resolution $\delta\omega$ of $\left[|Y(\omega)|^2\right]$ is comparable with the bandwidth $\Delta\omega$, the fine structures of $S_{xx}(\omega)$ in Eq. (26) are smoothed out, giving rise to a well-behaved peak for $\left[|Y(\omega)|^2\right]$ centered at $\omega = \tilde{\omega}_c$. This can be achieved by choosing $T_M = 1/\alpha$. The cavity resonance frequency can then determined by the the frequency corresponding to the center of the peak in $\left[|Y(\omega)|^2\right]_{\delta\omega=2\pi\alpha}$.

Numerical Results

In the current problem we intend to have low-pass filtered signal $x(t) = e^{i\phi(t)}$ for $0 < t < 10$ ms. The required bandwidth limit is $f_b = 5$ kHz ($f_b = \omega_b/2\pi$) and thus $T_b = 100$ μs. Two uniform random series u_n and v_n were generated for $n = (-200, 300)$, or $t = (-20, 30)$ ms, and $x(t)$ with the time interval $\Delta t = 10$ μs is evaluated for $0 < t < 10$ ms using Eqs. (2), (3) and (5). Figure 2 shows that $x(t)$ is a very good approximation of an ideal bandwidth-limited process. The simulation of the cavity response signal was obtained by numerical integration using Eq. (13), with given relative cavity resonance frequency $\tilde{f}_c \equiv f_c - f_0$. By setting the cut-off time $T_M = 1/\alpha = 1.4$ ms in Eq. (24) (for $Q_c = 6.6 \times 10^6$), the power spectrum of $y(t)$ is obtained as shown in Fig. 3. It shows that the central peak is well behaved and centered right at the given $\tilde{f}_c$. The residual spectrum away from the central peak is caused by the remaining oscillations of the factor $W_{T_M}(\omega - \omega')$ in Eq. (26).

The above simulation shows that the cavity resonance frequency can be revealed from the location of the central peak of the properly averaged power spectrum $|Y(\omega)|^2$ for the output signal $y(t)$. For the particular problem we are interested in, the cavity quality number Q_c is high enough that the output signal $y(t)$ is a sinusoidal signal with varying amplitude. The frequency of Re[$y(t)$] or Im[$y(t)$] determines the frequency offset from the operating frequency, and the direction of rotation of the vector $y(t)$ indicates whether it is a positive or negative frequency offset. The validity of the scheme presented in this paper is currently under test by experiments.

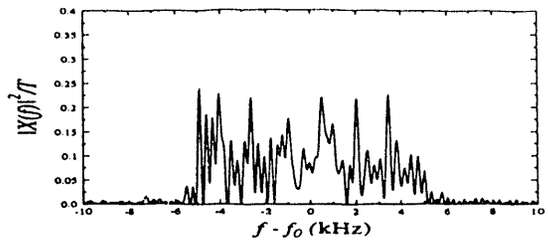

Figure 2: Power spectrum for the input signal $x(t)$.

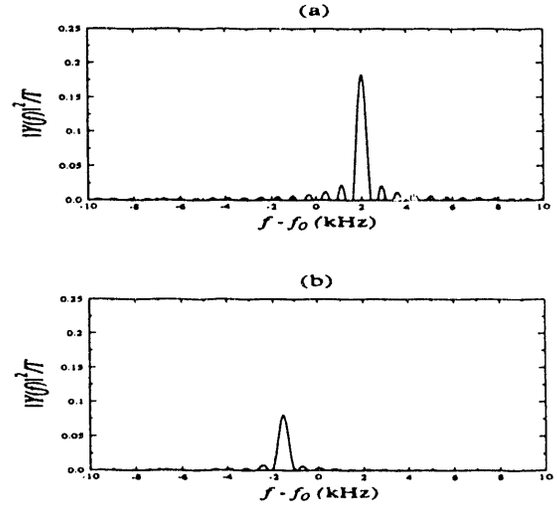

Figure 3: Power spectrum for the output signal $y(t)$ for (a) $\tilde{f}_c = 2$ kHz and (b) $\tilde{f}_c = -1.6$ kHz.

Acknowledgement

We wish to thank J. Bisognano for valuable discussions. The information provided by P. Gupta is also gratefully acknowledged.

References

[1] A. Papoulis, *Probability, Random Variables, and Stochastic Process*, 1965.

[2] G. M. Jenkins and D. G. Watts, *Spectral Analysis and its Applications*, 1968.

END

DATE FILMED

11/01/93